A New Formulation of Distribution Network Reconfiguration for Reducing the Voltage Volatility Induced by Distributed Generation

Yue Song, *Member, IEEE,* Yu Zheng, *Member, IEEE,* Tao Liu, *Member, IEEE,* Shunbo Lei, *Member, IEEE,* and David J. Hill, *Life Fellow, IEEE*

***Abstract*—Volatile voltage profiles in distribution systems caused by the fluctuating nature of renewable distributed generation (DG) are attracting growing concern. In this paper we develop a new formulation of network reconfiguration to mitigate voltage volatility. It provides new insights into the voltage regulation problem in distribution systems with high renewable penetration, which is commonly addressed by power electronic controllers. From the linear DistFlow equations, we first propose a novel index that measures the voltage volatility of each bus in the system. This index is a function of distribution network parameters that characterizes the role of network structure in voltage volatility. Then, we formulate a new reconfiguration model that minimizes the network loss and restricts the voltage volatility indices with the coordination of switched capacitor banks. A Benders decomposition-based approach is designed to solve the problem using mixed-integer quadratic programming. The simulations on the IEEE 69-bus system show that the reconfiguration scheme is able to: 1) minimize network loss when DG outputs are as predicted; and 2) significantly reduce the risk of voltage violations when DG outputs deviate from the prediction. The proposed formulation unleashes the distinctive power of network reconfiguration in reducing voltage volatility, by which the cost of power electronic controllers can be saved.**

***Index Terms*—distribution network reconfiguration, voltage volatility, distributed generation, linear DistFlow, mixed-integer quadratic programming**

I. Introduction

Distribution network reconfiguration refers to changing the operating structure of a distribution system while maintaining radial topology by resetting the status of line switches [1]. Reconfiguration is a common way for improving the performance of traditional distribution systems, where the load consumption is fed by substations only and operating scenarios can be described by several representative ones. The typical objectives of network reconfiguration include network loss minimization [2, 3], voltage regulation [4, 5], load balancing [1] and reliability enhancement [6], which have been extensively studied.

Nevertheless, the increasing penetration of renewable distributed generation (DG), such as wind and solar resources, has significantly changed the characteristics of distribution systems. The operating scenarios are becoming much more fluctuating due to the uncertain nature of DG outputs, which may induce volatile bus voltages. For example, it has been reported that the policies in Europe and United States that encourage the integration of photovoltaic units could cause significant voltage fluctuations along feeders [7, 8]. It indicates that a reconfiguration scheme, which well regulates the voltage profile under a predicted scenario, may still have unsatisfactory performance regarding bus voltages when the DG outputs deviate from the prediction. In addition, the response speed of network reconfiguration may be too slow to keep up with the fluctuation of DG outputs. Hence, network reconfiguration is commonly regarded as obsolete in the voltage regulation of distribution systems with high renewable penetration. Instead, in the existing reconfiguration models, the DG outputs are usually assumed controllable by, e.g., power curtailment [9, 10], which leads to the under-utilization of renewable energy.

Due to the fast response speed, power electronic controllers, such as distribution FACTS devices [11], DG inverters [12] and electric springs [13], have gained popularity in handling voltage volatility. Despite their satisfactory performance, the investment on power electronic voltage controllers is high so that careful planning is required. On the other hand, some existing results show that the voltage volatility problem is closely linked to distribution network structure. For example, it is empirically shown in [14] that a bus will have less severe voltage fluctuation if it locates closer to the substation or shares shorter conductors with photovoltaic units from the substation. In addition, an upper bound for voltage-power sensitivity is established in [15, 16], indicating that the impedance of such shared conductors plays an important role. These results hint that network reconfiguration, which is an existing tool in distribution systems, may effectively address the voltage volatility problem if carried out in a proper way. Following this idea, the role of network topology in voltage volatility needs further study to tap the potential of distribution network

This work was supported in part by the Hong Kong RGC General Research Fund under Project 17208817, in part by the Hong Kong RGC Theme-based Research Scheme under Project T23-701/14-N, in part by the National Natural Science Foundation of China under Grant 71801021, and in part by the Training Program of the Major Research Plan of the National Natural Science Foundation of China under Grant 91746118. *(Corresponding author: Yu Zheng)*

Y. Song and T. Liu are with the Department of Electrical and Electronic Engineering, The University of Hong Kong, Hong Kong (e-mail: yuesong@eee.hku.hk; taoliu@eee.hku.hk).

Y. Zheng is with the School of Electrical and Information Engineering, Changsha University of Science and Technology, Changsha 410004, China, and also with the Department of Electrical and Electronic Engineering, The University of Hong Kong, Hong Kong (e-mail: zhy9639@hotmail.com).

S. Lei is with the Department of Electrical Engineering and Computer Science, University of Michigan, Ann Arbor, MI, 48109 USA (email: shunbol@umich.edu).

D. J. Hill is with the Department of Electrical and Electronic Engineering, The University of Hong Kong, Hong Kong, and also with the School of Electrical and Information Engineering, The University of Sydney, Sydney, NSW 2006, Australia (e-mail: dhill@eee.hku.hk; david.hill@sydney.edu.au).

reconfiguration.

In this paper, we analytically reveal the relationship between the DG-induced voltage volatility and distribution network structure, and establish a new reconfiguration formulation that reduces voltage volatility level. The main contributions are twofold. First, we propose a new index to measure the voltage volatility of a bus based on the linear DistFlow equations. The index is a function of distribution network parameters that concisely describes the degree of voltage fluctuation with DG outputs. Second, we develop a new reconfiguration strategy with the coordination of the switched capacitor banks (CBs)—another common device with slow response, which minimizes the network loss for the predicted scenario and restricts the voltage volatility indices. The proposed model is solved by the Benders decomposition-based method, where the problem for each iteration is a mixed-integer quadratic program (MIQP). Also we adopt some simple linear constraints for imposing network radiality, which reduces the problem dimension. The obtained reconfiguration scheme achieves high economy when DG outputs are as predicted, and low risk of voltage violations when DG outputs deviate from the prediction. From these results, we discover the distinctive capability of network reconfiguration in addressing the voltage volatility problem.

The rest of the paper is organized as follows. Section II provides some preliminaries and the linear DistFlow equations as a basis. The voltage volatility index is proposed in Section III based on the linear DistFlow. In Section IV, the network reconfiguration problem considering voltage volatility constraints is formulated and a Benders decomposition-based algorithm is designed. Section V gives numerical tests to verify the proposed method, and Section VI makes a conclusion and a prospect for future works.

II. Power flow model in distribution systems

A. Notations and graph theory preliminaries

For simplicity, a vector $\boldsymbol{x} = [x_1, x_2, ..., x_p]^T \in \mathbb{R}^p$ is denoted as $\boldsymbol{x} = [x_i] \in \mathbb{R}^p$, and a diagonal matrix $\boldsymbol{A} = \text{diag}\{a_1, a_2, ..., a_p\} \in \mathbb{R}^{p\times p}$ is denoted as $\boldsymbol{A} = \text{diag}\{a_i\} \in \mathbb{R}^{p\times p}$. We slightly abuse the notation $|\cdot|$, using it to denote the cardinality when applying to a set and the entry-wise absolute value when applying to a matrix. The notation $\mathbf{1}_p \in \mathbb{R}^p$ denotes the vector with all entries being one. For two vectors $\boldsymbol{x}, \boldsymbol{y} \in \mathbb{R}^p$, the notation $\boldsymbol{x} \leq \boldsymbol{y}$ represents the entry-wise inequality $x_i \leq y_i$, $i = 1, 2, ..., p$.

We also introduce some graph theory preliminaries as a basis (referring to [17] for the details). Denote an undirected graph as $\mathcal{G}(\mathcal{V}, \mathcal{E})$ where $\mathcal{V}$ is the set of nodes and $\mathcal{E} \subseteq \mathcal{V} \times \mathcal{V}$ is the set of edges with $|\mathcal{V}| = n$ and $|\mathcal{E}| = l$. The notation $e_k = (i, j) \in \mathcal{E}$, $k = 1, 2, .., l$, denotes the edge k that connects node i and node j, where (i, j) denotes an unordered node pair. To define the incidence matrix, each edge of $\mathcal{G}$ is fictitiously assigned a fixed orientation, e.g., $e_k = (i, j)$ is assumed to originate at node i and terminate at node j. Then, the incidence matrix $\boldsymbol{E} \in \mathbb{R}^{n\times l}$ is defined such that $\forall e_k = (i, j) \in \mathcal{E}$, $E_{ik} = 1$, $E_{jk} = -1$ and $E_{mk} = 0, m \neq i, j$. A path in a graph refers to a set of edges that connect a sequence of nodes which are all distinct from one another, except that the starting node and ending node are possibly the same. A tree refers to an undirected graph where any two nodes are connected by exactly one path. For a connected graph $\mathcal{G}$, a spanning tree refers to a subgraph of $\mathcal{G}$ that is a tree containing every node of $\mathcal{G}$, denoted as $\mathcal{T}(\mathcal{V}, \mathcal{E}_\mathcal{T})$ with $\mathcal{E}_\mathcal{T} \subseteq \mathcal{E}$ and $|\mathcal{E}_\mathcal{T}| = n - 1$. For a graph $\mathcal{G}$ with c connected components, a spanning forest refers to a subgraph of $\mathcal{G}$ that consists of a spanning tree in each connected component of $\mathcal{G}$, denoted as $\mathcal{F}(\mathcal{V}, \mathcal{E}_\mathcal{F})$ with $\mathcal{E}_\mathcal{F} \subseteq \mathcal{E}$ and $|\mathcal{E}_\mathcal{F}| = n - c$.

B. Linear DistFlow equations

Consider a distribution system with the set of buses $\mathcal{V}$ and set of lines[1] $\mathcal{E}$. The system is assumed to be three-phase balanced and a per-phase analysis is carried out. The bus set $\mathcal{V}$ consists of two subsets $\mathcal{V}_s$ and $\mathcal{V}_d$ with $|\mathcal{V}_s| = s$ and $|\mathcal{V}_d| = d$, where $\mathcal{V}_s$ denotes the set of substations and $\mathcal{V}_d = \mathcal{V}\backslash\mathcal{V}_s$ denotes the set of the non-substation buses that may connect loads and DGs. Without loss of generality, we assume $\mathcal{V}_d = \{1, 2, ..., d\}$ and $\mathcal{V}_s = \{d + 1, ..., d + s\}$. The line set $\mathcal{E}$ consists of two subsets $\mathcal{E}_{sw}$ and $\mathcal{E}_{on}$, where $\mathcal{E}_{sw}$ denotes the set of switchable lines and $\mathcal{E}_{on} = \mathcal{E}\backslash\mathcal{E}_{sw}$ denotes the set of the remaining lines being always on. As a convention, assume the distribution system operates with a radial network topology, i.e., the line status should guarantee that each bus $i \in \mathcal{V}_d$ is connected to a unique substation by exactly one path of lines. In other words, an operating distribution network can be regarded as a spanning forest $\mathcal{F}(\mathcal{V}, \mathcal{E}_\mathcal{F})$ with $\mathcal{E}_\mathcal{F} \subseteq \mathcal{E}$, $|\mathcal{E}_\mathcal{F}| = d$, which consists of s trees with each tree containing a unique substation.

For each bus $i \in \mathcal{V}$, denote V_i, θ_i as the voltage magnitude and phase angle, and P_i, Q_i as the active and reactive power injection (i.e., DG output minus load). For each line $(i, j) \in \mathcal{E}$, denote r_{ij}, x_{ij} as the resistance and reactance, P_{ij}, Q_{ij} as the sending-end active power and reactive power from bus i to bus j, and l_{ij} as squared magnitude of line current. Given an operating distribution network $\mathcal{F}(\mathcal{V}, \mathcal{E}_\mathcal{F})$, we have the following equations with respect to each line $(i, j) \in \mathcal{E}_\mathcal{F}$

$$S_{ij} - (r_{ij} + \mathrm{j}x_{ij})l_{ij} + S_j + \sum\nolimits_{k\in\mathcal{N}_\mathcal{F}^j\backslash\{i\}} S_{jk} = 0 \quad (1a)$$

$$V_i\angle\theta_i - (r_{ij} + \mathrm{j}x_{ij})S_{ij}^*/(V_i\angle\theta_i)^* = V_j\angle\theta_j \quad (1b)$$

$$l_{ij} = |S_{ij}/V_i|^2 \quad (1c)$$

where $S_j = P_j + \mathrm{j}Q_j$ denotes the complex power injection; $S_{ij} = P_{ij} + \mathrm{j}Q_{ij}$ denotes the complex line flow at the sending-end; $V_i\angle\theta_i$ denotes the complex bus voltage; $\mathcal{N}_\mathcal{F}^j$ denotes the set of neighboring buses of bus j in the network $\mathcal{F}(\mathcal{V}, \mathcal{E}_\mathcal{F})$, $i \in \mathcal{N}_\mathcal{F}^j$ means line (i, j) is switched on in the network $\mathcal{F}$; and the superscript * means the conjugate of a complex number. Equation (1a) describes the power balance at bus j, (1b) describes the voltage drop along line (i, j), and (1c) describes the relationship between line current and line flow. Reformulating (1) in terms of real variables gives the DistFlow

[1]Due to the terminology convention, we will interchangeably use "bus, line" for distribution systems and "node, edge" for graphs henceforth.

equations [1]

$$P_{ij} = -P_j + r_{ij}l_{ij} + \sum\nolimits_{k\in\mathcal{N}_{\mathcal{F}}^j\setminus\{i\}} P_{jk} \tag{2a}$$

$$Q_{ij} = -Q_j + x_{ij}l_{ij} + \sum\nolimits_{k\in\mathcal{N}_{\mathcal{F}}^j\setminus\{i\}} Q_{jk} \tag{2b}$$

$$V_i^2 - V_j^2 = 2(r_{ij}P_{ij} + x_{ij}Q_{ij}) - (r_{ij}^2 + x_{ij}^2)l_{ij} \tag{2c}$$

$$l_{ij}V_i^2 = P_{ij}^2 + Q_{ij}^2 \tag{2d}$$

where (2a) and (2b) follow from (1a), (2c) is given by taking magnitude squared of (1b), and (2d) is given by (1c).

The nonlinear DistFlow equations can be simplified into a linear version by utilizing some operational properties of distribution systems. First, the terms $r_{ij}l_{ij}, x_{ij}l_{ij}$, which refer to line loss, are much smaller than line flow terms P_{ij}, Q_{ij}. For instance, the maximum ratio of line loss to line flow is less than 8% for all three network configurations of IEEE 69-bus system used in case study (see Section V). So we can drop $r_{ij}l_{ij}$ in (2a), $x_{ij}l_{ij}$ in (2b) and $(r_{ij}^2 + x_{ij}^2)l_{ij}$ in (2c), and no longer care about (2d) as it becomes trivial in power flow. In addition, we have the approximation $V_i^2 - V_j^2 = 2(V_i - V_j)$ since $V_i \simeq 1$, which introduces a small relative error of around 0.25% (1%) if there is 5% (10%) deviation in voltage magnitude [12]. These manipulations lead to the linear DistFlow equations below, which has been established in [1, 12]

$$P_i = \sum\nolimits_{k\in\mathcal{N}_{\mathcal{F}}^i} P_{ik} \tag{3a}$$

$$Q_i = \sum\nolimits_{k\in\mathcal{N}_{\mathcal{F}}^i} Q_{ik} \tag{3b}$$

$$V_i - V_j = r_{ij}P_{ij} + x_{ij}Q_{ij}. \tag{3c}$$

We will study voltage volatility and network reconfiguration using (3) as it concisely describes the voltage-power relationship in distribution systems.

III. Definition of voltage volatility index

We first reformulate the linear DistFlow euqations by graph-related matrices. Denote $\boldsymbol{E}_{\mathcal{F}} \in \mathbb{R}^{(d+s)\times d}$ as the incidence matrix of the operating distribution network $\mathcal{F}(\mathcal{V}, \mathcal{E}_{\mathcal{F}})$, where each switch-on line (i, j) is fictitiously assigned the orientation from bus i to bus j. The matrix $\boldsymbol{E}_{\mathcal{F}}$ can be partitioned into $\boldsymbol{E}_{\mathcal{F}} = \begin{bmatrix}\boldsymbol{E}_{\mathcal{F},d}^T & \boldsymbol{E}_{\mathcal{F},s}^T\end{bmatrix}^T$, where $\boldsymbol{E}_{\mathcal{F},d} \in \mathbb{R}^{d\times d}$ and $\boldsymbol{E}_{\mathcal{F},s} \in \mathbb{R}^{s\times d}$ denotes the sub-matrices of $\boldsymbol{E}_{\mathcal{F}}$ whose rows are indexed by $\mathcal{V}_d$ and $\mathcal{V}_s$, respectively. Also, we introduce the voltage vectors $\boldsymbol{V}_d = [V_i] \in \mathbb{R}^d$, $\forall i \in \mathcal{V}_d$ and $\boldsymbol{V}_s = [V_i] \in \mathbb{R}^s$, $\forall i \in \mathcal{V}_s$, power injection vectors $\boldsymbol{P}_d = [P_i], \boldsymbol{Q}_d = [Q_i] \in \mathbb{R}^d$, $\forall i \in \mathcal{V}_d$, line flow vectors $\boldsymbol{P}_{\mathcal{E}_{\mathcal{F}}} = [P_{ij}]$, $\boldsymbol{Q}_{\mathcal{E}_{\mathcal{F}}} = [Q_{ij}] \in \mathbb{R}^d$, $\forall (i, j) \in \mathcal{E}_{\mathcal{F}}$ and the diagonal matrices $\boldsymbol{r}_{\mathcal{E}_{\mathcal{F}}} = \text{diag}\{r_{ij}\}, \boldsymbol{x}_{\mathcal{E}_{\mathcal{F}}} = \text{diag}\{x_{ij}\} \in \mathbb{R}^{d\times d}$, $\forall (i, j) \in \mathcal{E}_{\mathcal{F}}$. Then, equation (3) can be re-expressed as

$$\boldsymbol{P}_d = \boldsymbol{E}_{\mathcal{F},d}\boldsymbol{P}_{\mathcal{E}_{\mathcal{F}}} \tag{4a}$$

$$\boldsymbol{Q}_d = \boldsymbol{E}_{\mathcal{F},d}\boldsymbol{Q}_{\mathcal{E}_{\mathcal{F}}} \tag{4b}$$

$$\boldsymbol{E}_{\mathcal{F},d}^T\boldsymbol{V}_d + \boldsymbol{E}_{\mathcal{F},s}^T\boldsymbol{V}_s = \boldsymbol{r}_{\mathcal{E}_{\mathcal{F}}}\boldsymbol{P}_{\mathcal{E}_{\mathcal{F}}} + \boldsymbol{x}_{\mathcal{E}_{\mathcal{F}}}\boldsymbol{Q}_{\mathcal{E}_{\mathcal{F}}}. \tag{4c}$$

where $\boldsymbol{E}_{\mathcal{F},d}$ is nonsingular since the distribution network is radial [17]. Then we have $\boldsymbol{P}_{\mathcal{E}_{\mathcal{F}}} = \boldsymbol{E}_{\mathcal{F},d}^{-1}\boldsymbol{P}_d$ and $\boldsymbol{Q}_{\mathcal{E}_{\mathcal{F}}} = \boldsymbol{E}_{\mathcal{F},d}^{-1}\boldsymbol{Q}_d$ from (4a) and (4b), and substituting them into (4c) gives

$$\boldsymbol{V}_d = \boldsymbol{R}\boldsymbol{P}_d + \boldsymbol{X}\boldsymbol{Q}_d + \boldsymbol{V}_d^0 \tag{5}$$

where $\boldsymbol{V}_d^0 = -(\boldsymbol{E}_{\mathcal{F},d}^{-1})^T\boldsymbol{E}_{\mathcal{F},s}^T\boldsymbol{V}_s \in \mathbb{R}^d$ is a constant vector as the substations keep constant voltages and

$$\begin{aligned}\boldsymbol{R} &= (\boldsymbol{E}_{\mathcal{F},d}^{-1})^T\boldsymbol{r}_{\mathcal{E}_{\mathcal{F}}}\boldsymbol{E}_{\mathcal{F},d}^{-1} \in \mathbb{R}^{d\times d}\\ \boldsymbol{X} &= (\boldsymbol{E}_{\mathcal{F},d}^{-1})^T\boldsymbol{x}_{\mathcal{E}_{\mathcal{F}}}\boldsymbol{E}_{\mathcal{F},d}^{-1} \in \mathbb{R}^{d\times d}.\end{aligned} \tag{6}$$

Note that $\boldsymbol{R}^{-1}$ and $\boldsymbol{X}^{-1}$ coincide with the conductance matrix and susceptance matrix of the distribution network, respectively. Furthermore, the radiality of distribution networks leads to an explicit expression for the entries of $\boldsymbol{R}$ and $\boldsymbol{X}$. In the network $\mathcal{F}(\mathcal{V}, \mathcal{E}_{\mathcal{F}})$, denote $\mathcal{H}_{\mathcal{F}}^i$ as the set of lines contained in the path from bus i to the substation that bus i connects to. According to [12], the (i, j) entry of $\boldsymbol{R}$ and $\boldsymbol{X}$, say R_{ij} and X_{ij}, can be expressed by

$$R_{ij} = \begin{cases} \sum_{(k,l)\in\mathcal{H}_{\mathcal{F}}^i} r_{kl}, & i = j\\ \sum_{(k,l)\in\mathcal{H}_{\mathcal{F}}^i\cap\mathcal{H}_{\mathcal{F}}^j} r_{kl}, & i \neq j.\end{cases} \tag{7}$$

$$X_{ij} = \begin{cases} \sum_{(k,l)\in\mathcal{H}_{\mathcal{F}}^i} x_{kl}, & i = j\\ \sum_{(k,l)\in\mathcal{H}_{\mathcal{F}}^i\cap\mathcal{H}_{\mathcal{F}}^j} x_{kl}, & i \neq j.\end{cases} \tag{8}$$

We now consider the situation where the DG outputs are fluctuating. Let $\mathcal{V}_{dg} \subseteq \mathcal{V}_d$ be the set of buses that install DGs. Then, we have the incremental form of (5) that describes how bus voltages fluctuate with DG outputs

$$\Delta\boldsymbol{V}_d = \boldsymbol{R}_{dg}\Delta\boldsymbol{P}_{dg} + \boldsymbol{X}_{dg}\Delta\boldsymbol{Q}_{dg} \tag{9}$$

where $\Delta\boldsymbol{P}_{dg} = [\Delta P_i]$, $\Delta\boldsymbol{Q}_{dg} = [\Delta Q_i] \in \mathbb{R}^{|\mathcal{V}_{dg}|}$, $\forall i \in \mathcal{V}_{dg}$ represent the deviations from the predicted values, and $\boldsymbol{R}_{dg}, \boldsymbol{X}_{dg} \in \mathbb{R}^{d\times|\mathcal{V}_{dg}|}$ denote the sub-matrices of $\boldsymbol{R}$ and $\boldsymbol{X}$ whose columns are indexed by $\mathcal{V}_{dg}$. In the following we rewrite each row of (9) that helps to understand the mechanism of voltage fluctuation

$$\Delta V_i = \sum\nolimits_{j\in\mathcal{V}_{dg}} R_{ij}\Delta P_j + X_{ij}\Delta Q_j,\ i \in \mathcal{V}_d. \tag{10}$$

Equation (10) implies that the distribution network works as an "amplifier" that couples power fluctuations to bus voltages. For the voltage deviation at bus i caused by the power fluctuation at bus j, the amplifications R_{ij}, X_{ij} are determined by the total resistances and reactances of the lines shared by the path from bus i to the substation and the path from bus j to the substation. A larger R_{ij} (or X_{ij}) implies that the voltage of bus i is more volatile to the active (or reactive) power fluctuation at bus j.

Based on (10), we establish the voltage volatility index of bus $i \in \mathcal{V}_d$ as follows

$$\mathcal{I}_i = \sum\nolimits_{j\in\mathcal{V}_{dg}} R_{ij} + X_{ij} = \boldsymbol{e}_i^T(\boldsymbol{R} + \boldsymbol{X})\boldsymbol{e}_{dg} \tag{11}$$

where $\boldsymbol{e}_i \in \mathbb{R}^d$ denotes the vector with the i-th entry being one and the other entries being zero; $\boldsymbol{e}_{dg} = [e_{dgi}] \in \mathbb{R}^d$ is defined such that $e_{dgi} = 1$, $\forall i \in \mathcal{V}_{dg}$ and $e_{dgi} = 0$, $\forall i \in \mathcal{V}_d \setminus \mathcal{V}_{dg}$. Note that the load-induced voltage volatility is not considered in the analysis as the uncertainties of loads are usually smaller than those of DGs [18]. Nevertheless, it will not impact the generality of the voltage volatility index. If some loads do have large fluctuations, we can include the corresponding buses into the set $\mathcal{V}_{dg}$ and similar results can be obtained.

We further explain the physical meaning of $\mathcal{I}_i$. It follows from (9) and (11) that

$$\max_{i\in\mathcal{V}_d} \mathcal{I}_i = \left\| \begin{bmatrix} \boldsymbol{R}_{dg} & \boldsymbol{X}_{dg} \end{bmatrix} \right\|_\infty = \sup_{\Delta \boldsymbol{S}_{dg}\neq \boldsymbol{0}} \frac{\|\Delta \boldsymbol{V}_d\|_\infty}{\|\Delta \boldsymbol{S}_{dg}\|_\infty} \quad (12)$$

where $\|\cdot\|_\infty$ denotes the ∞-norm of a matrix, $\sup\{\cdot\}$ denotes the supremum of a set, and $\Delta \boldsymbol{S}_{dg} = \begin{bmatrix} \Delta \boldsymbol{P}_{dg}^T & \Delta \boldsymbol{Q}_{dg}^T \end{bmatrix}^T$. By (12), the maximum $\mathcal{I}_i$ in the system characterizes the maximum ratio of bus voltage deviation to DG output fluctuation under ∞-norm. Hence, the index $\mathcal{I}_i$ gives a proper measure of voltage volatility. A lower $\mathcal{I}_i$ implies the voltage of bus i is more robust against power fluctuations.

The proposed index $\mathcal{I}_i$ also provides a quantified explanation for some empirical observations. It is shown in [14] that bus i has less severe voltage fluctuation if it is closer to the substation or has shorter shared conductors with DGs from the substation. By (7) and (8), locating closer to the substation implies a smaller R_{ii} and X_{ii}, and shorter shared conductors with DGs implies a smaller R_{ij} and X_{ij}, $j \in \mathcal{V}_{dg}$, both of which induce a smaller $\mathcal{I}_i$ and hence less voltage volatility of bus i.

Moreover, it needs to be emphasized that the above analysis implies voltage-power sensitivities are strongly but not exclusively related to network topology. The actual voltage-power sensitivities depend on both network topology and system states (bus voltage magnitudes and phase angles), e.g., see an analysis in [15, 16] that gives an upper bound for voltage-power sensitivity. The proposed index $\mathcal{I}_i$ has a more focused consideration; it aims at getting a specifically simplified form as a function of R_{ij}, X_{ij} that explicitly reveals the role of network topology in voltage volatility. This leads to a clear indication that network reconfiguration is an effective way for reducing voltage volatility if the switch actions are regulated by the index $\mathcal{I}_i$.

Take Fig. 1 as an illustrative example that shows how network reconfiguration mitigates voltage volatility. Assume bus j has fluctuating DG output and R_{ij} is large. Then the left configuration in Fig. 1 leads to a volatile voltage profile at bus i. By comparison, the right configuration significantly reduces the voltage volatility of bus i as it shares no lines with bus j from the substation. In the next section, a systematic formulation will be developed based on this idea.

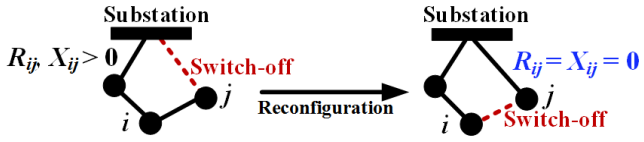

Figure 1. An example of voltage volatility mitigation via reconfiguration.

IV. Voltage Volatility Constrained Network Reconfiguration

A. Optimization problem formulation

As shown in the previous section, distribution network structure plays an important role in determining voltage volatility. For the network reconfiguration that focuses on loss reduction only, the voltage volatility level may be increased so that voltage violation is more likely to occur in case of DG output fluctuations, an example of which will be seen in the case study. On the other hand, a robust voltage profile can be achieved by the reconfiguration with voltage volatility indices being well-bounded, which could also alleviate the burden of corrective control given by power-electronic voltage controllers. From this motivation, we propose a new framework where network reconfiguration coordinates with the switched CBs, whose response speed is similar to reconfiguration, to address the network loss, voltage regulation and voltage volatility issues.

We introduce the following notations before presenting the mathematical model

$$\begin{aligned}
&\boldsymbol{P}_d^{pre} = [P_i^{pre}] \in \mathbb{R}^d,\ \forall i \in \mathcal{V}_d \\
&\boldsymbol{Q}_d^{pre} = [Q_i^{pre}] \in \mathbb{R}^d,\ \forall i \in \mathcal{V}_d \\
&\boldsymbol{U}^{cb} = \text{diag}\{U_i^{cb}\} \in \mathbb{R}^{d\times d},\ \forall i \in \mathcal{V}_d \\
&\boldsymbol{c} = [c_i] \in \mathbb{R}^d,\ \forall i \in \mathcal{V}_d \\
&\boldsymbol{r}_{\mathcal{E}} = \text{diag}\{r_{ij}\} \in \mathbb{R}^{l\times l},\ \forall (i,j) \in \mathcal{E} \\
&\boldsymbol{x}_{\mathcal{E}} = \text{diag}\{x_{ij}\} \in \mathbb{R}^{l\times l},\ \forall (i,j) \in \mathcal{E} \\
&\boldsymbol{P}_{\mathcal{E}} = \text{diag}\{P_{ij}\} \in \mathbb{R}^{l},\ \forall (i,j) \in \mathcal{E} \\
&\boldsymbol{Q}_{\mathcal{E}} = \text{diag}\{Q_{ij}\} \in \mathbb{R}^{l},\ \forall (i,j) \in \mathcal{E} \\
&\boldsymbol{\alpha} = [\alpha_{ij}] \in \mathbb{R}^{l},\ \forall (i,j) \in \mathcal{E}
\end{aligned} \quad (13)$$

where P_i^{pre}, Q_i^{pre} denote the predicted power injections given by the DG and load forecast; U_i^{cb} denotes the unit size of the CB at bus i; c_i is an integer variable representing the position level of the CB at bus i; and α_{ij} is a binary variable indicating line status, $\alpha_{ij} = 1$ represents line (i,j) is switched on, and $\alpha_{ij} = 0$ represents line (i,j) is switched off.

Moreover, we derive another expression of $\mathcal{I}_i$ for the convenience of reconfiguration model formulation. Denote $\mathcal{G}(\mathcal{V},\mathcal{E})$ as the entire graph structure of the distribution system including both the switch-on and switch-off lines. Let $\boldsymbol{E}_{\mathcal{G}} = \begin{bmatrix} \boldsymbol{E}_{\mathcal{G},d}^T & \boldsymbol{E}_{\mathcal{G},s}^T \end{bmatrix}^T \in \mathbb{R}^{(d+s)\times l}$ be the incidence matrix of $\mathcal{G}(\mathcal{V},\mathcal{E})$, where $\boldsymbol{E}_{\mathcal{G},d} \in \mathbb{R}^{d\times l}$ and $\boldsymbol{E}_{\mathcal{G},s} \in \mathbb{R}^{s\times l}$ denotes the sub-matrices whose rows are indexed by $\mathcal{V}_d$ and $\mathcal{V}_s$, respectively. Then, the matrices $\boldsymbol{R}$ and $\boldsymbol{X}$ defined in (6) can be re-expressed in terms of network configuration $\boldsymbol{\alpha}$

$$\begin{aligned}
\boldsymbol{R}(\boldsymbol{\alpha}) &= [\boldsymbol{E}_{\mathcal{G},d}\boldsymbol{g}_{\mathcal{E}}(\boldsymbol{\alpha})\boldsymbol{E}_{\mathcal{G},d}^T]^{-1} \\
\boldsymbol{X}(\boldsymbol{\alpha}) &= [\boldsymbol{E}_{\mathcal{G},d}\boldsymbol{b}_{\mathcal{E}}(\boldsymbol{\alpha})\boldsymbol{E}_{\mathcal{G},d}^T]^{-1}
\end{aligned} \quad (14)$$

where $\boldsymbol{g}_{\mathcal{E}}(\boldsymbol{\alpha}) = \text{diag}\{r_{ij}^{-1}\alpha_{ij}\}$, $\boldsymbol{b}_{\mathcal{E}}(\boldsymbol{\alpha}) = \text{diag}\{x_{ij}^{-1}\alpha_{ij}\} \in \mathbb{R}^{l\times l}$ with $\alpha_{ij} = 1$ if $(i,j) \in \mathcal{E}_{\mathcal{F}}$ and $\alpha_{ij} = 0$ otherwise. Thus, the voltage volatility index defined in (11) can be re-expressed as a function of $\boldsymbol{\alpha}$

$$\begin{aligned}
\mathcal{I}_i(\boldsymbol{\alpha}) &= \boldsymbol{e}_i^T[\boldsymbol{R}(\boldsymbol{\alpha}) + \boldsymbol{X}(\boldsymbol{\alpha})]\boldsymbol{e}_{dg} \\
&= \boldsymbol{e}_i^T\{[\boldsymbol{E}_{\mathcal{G},d}\boldsymbol{g}_{\mathcal{E}}(\boldsymbol{\alpha})\boldsymbol{E}_{\mathcal{G},d}^T]^{-1} + [\boldsymbol{E}_{\mathcal{G},d}\boldsymbol{b}_{\mathcal{E}}(\boldsymbol{\alpha})\boldsymbol{E}_{\mathcal{G},d}^T]^{-1}\}\boldsymbol{e}_{dg}.
\end{aligned} \quad (15)$$

With these notations, the network reconfiguration problem

considering voltage volatility constraints is formulated as

$$\min_{\boldsymbol{\alpha},\boldsymbol{c},\boldsymbol{P}_\mathcal{E},\boldsymbol{Q}_\mathcal{E},\boldsymbol{V}_d} \quad \boldsymbol{P}_\mathcal{E}^T \boldsymbol{r}_\mathcal{E} \boldsymbol{P}_\mathcal{E} + \boldsymbol{Q}_\mathcal{E}^T \boldsymbol{r}_\mathcal{E} \boldsymbol{Q}_\mathcal{E} \tag{16a}$$

$$s.t.\ \boldsymbol{P}_d^{pre} = \boldsymbol{E}_{\mathcal{G},d} \boldsymbol{P}_\mathcal{E} \tag{16b}$$

$$\boldsymbol{Q}_d^{pre} + \boldsymbol{U}^{cb} \boldsymbol{c} = \boldsymbol{E}_{\mathcal{G},d} \boldsymbol{Q}_\mathcal{E} \tag{16c}$$

$$\boldsymbol{E}_{\mathcal{G},d}^T \boldsymbol{V}_d + \boldsymbol{E}_{\mathcal{G},s}^T \boldsymbol{V}_s \geq \boldsymbol{r}_\mathcal{E} \boldsymbol{P}_\mathcal{E} + \boldsymbol{x}_\mathcal{E} \boldsymbol{Q}_\mathcal{E} - M(\mathbf{1}_l - \boldsymbol{\alpha}) \tag{16d}$$

$$\boldsymbol{E}_{\mathcal{G},d}^T \boldsymbol{V}_d + \boldsymbol{E}_{\mathcal{G},s}^T \boldsymbol{V}_s \leq \boldsymbol{r}_\mathcal{E} \boldsymbol{P}_\mathcal{E} + \boldsymbol{x}_\mathcal{E} \boldsymbol{Q}_\mathcal{E} + M(\mathbf{1}_l - \boldsymbol{\alpha}) \tag{16e}$$

$$-\boldsymbol{P}_\mathcal{E}^{\max} \boldsymbol{\alpha} \leq \boldsymbol{P}_\mathcal{E} \leq \boldsymbol{P}_\mathcal{E}^{\max} \boldsymbol{\alpha} \tag{16f}$$

$$-\boldsymbol{Q}_\mathcal{E}^{\max} \boldsymbol{\alpha} \leq \boldsymbol{Q}_\mathcal{E} \leq \boldsymbol{Q}_\mathcal{E}^{\max} \boldsymbol{\alpha} \tag{16g}$$

$$\alpha_{ij} \in \{0,1\},\ \forall (i,j) \in \mathcal{E}_{sw} \tag{16h}$$

$$\alpha_{ij} = 1,\ \forall (i,j) \in \mathcal{E}_{on} \tag{16i}$$

$$c_i \in \mathcal{S}_{ci},\ \forall i \in \mathcal{V}_d \tag{16j}$$

$$\mathbf{1}_l^T \boldsymbol{\alpha} = d \tag{16k}$$

$$|\boldsymbol{E}_{\mathcal{G},s}| \boldsymbol{\alpha} \geq \mathbf{1}_s \tag{16l}$$

$$\boldsymbol{V}_d^{\min} \leq \boldsymbol{V}_d \leq \boldsymbol{V}_d^{\max} \tag{16m}$$

$$\mathcal{I}_i(\boldsymbol{\alpha}) \leq \mathcal{I}_i^{\max},\ \forall i \in \mathcal{V}_d \tag{16n}$$

where the quadratic objective function (16a) represents the network loss (it is a commonly used expression with the employment of $V_i \simeq 1$ [1]); M is a large positive constant; $\boldsymbol{P}_\mathcal{E}^{\max} = \text{diag}\{P_{ij}^{\max}\} \in \mathbb{R}^{l \times l}$, $\forall (i,j) \in \mathcal{E}$ with $P_{ij}^{\max}$ being the active power flow limit of line (i,j); $\boldsymbol{Q}_\mathcal{E}^{\max} = \text{diag}\{Q_{ij}^{\max}\} \in \mathbb{R}^{l \times l}$, $\forall (i,j) \in \mathcal{E}$ with $Q_{ij}^{\max}$ being the reactive power flow limit of line (i,j); $\mathcal{S}_{ci}$ denotes the feasible position levels of the CB at bus i; and $\mathcal{I}_i^{\max}$ denotes the upper bound for the voltage volatility index of bus i. The power injection equations (3a) and (3b) with respect to the substations are not included since the power fed by each substation is known only after the reconfiguration scheme is determined.

In the following we further explain some constraints in (16).

1) Power flow equations and disjunctive constraints (16b)-(16i). For $\alpha_{ij} = 1$, i.e., line (i,j) is switched on, the associated constraints in (16d) and (16e) are equivalent to (3c). Meanwhile, (16f) and (16g) enforce P_{ij}, Q_{ij} to take values within line flow limits. For $\alpha_{ij} = 0$, i.e., line (i,j) is switched off, the associated constraints in (16d) and (16e) are deactivated by the large number M, and P_{ij}, Q_{ij} are enforced to be zero by (16f) and (16g).

2) Voltage magnitude constraint (16m) and voltage volatility constraint (16n). These constraints work together to achieve a robust voltage profile. When the actual operating scenario is as predicted, the bus voltages are enforced to be close to the flat profile (1.0 p.u.) by (16m). When the actual operating scenario fluctuates from the prediction, the voltage deviation from the flat profile is well limited by (16n), and thus the risk of voltage violation is reduced. For those buses with higher volatility, tighter voltage bounds (e.g., 1 ± 0.03 p.u.) can be adopted in (16m) for a better control effect.

3) Constraints for network radiality (16k) and (16l). Constraint (16k) implies that the total number of switch-on lines is equal to d, which is a necessary condition for network radiality. Constraint (16l) implies that each substation is connected to at least one line. We show below that these constraints together with power flow constraints provide a necessary and sufficient condition for network radiality.

Theorem 1: Assume $\sum_{i \in \mathcal{V}_a} P_i^{pre} \neq 0$ for any arbitrary subset $\mathcal{V}_a \subset \mathcal{V}_d$. Then, network radiality is met by a network configuration $\boldsymbol{\alpha}$ if and only if it satisfies (16b), (16f), (16k) and (16l).

Proof: The necessity part is straightforward and we prove the sufficiency below.

Note that there are three types of network configurations satisfying (16k) and (16l). The first type refers to a desirable configuration. In the second type, there are isolated non-substation buses due to the existence of loops in the network, which is infeasible. In the third type, there are isolated non-substation buses due to multiple substations being contained in one connected component, which is also infeasible (see the examples in Fig. 2).

For the latter two types of configurations, let $\mathcal{V}_a \subset \mathcal{V}_d$ denote the set of isolated non-substation buses with $|\mathcal{V}_a| = a$, and $\boldsymbol{E}_{\mathcal{G},a} \in \mathbb{R}^{a \times l}$ denote the sub-matrix of $\boldsymbol{E}_\mathcal{G}$ whose rows are indexed by $\mathcal{V}_a$. Let $\boldsymbol{E}_{\mathcal{G},a}^1$ collect the columns of $\boldsymbol{E}_{\mathcal{G},a}$ indexed by the lines within $\mathcal{V}_a$, $\boldsymbol{E}_{\mathcal{G},a}^2$ collect the columns indexed by the lines between $\mathcal{V}_a$ and $\mathcal{V} \backslash \mathcal{V}_a$, and $\boldsymbol{E}_{\mathcal{G},a}^3$ collect the columns indexed by the lines within $\mathcal{V} \backslash \mathcal{V}_a$. Accordingly, let $\boldsymbol{P}_\mathcal{E}^1$ be the set of line flows within $\mathcal{V}_a$, $\boldsymbol{P}_\mathcal{E}^2$ be the set of line flows between $\mathcal{V}_a$ and $\mathcal{V} \backslash \mathcal{V}_a$, and $\boldsymbol{P}_\mathcal{E}^3$ be the set of line flows within $\mathcal{V} \backslash \mathcal{V}_a$. It is trivial to check that $\mathbf{1}_a^T \boldsymbol{E}_{\mathcal{G},a}^1 = \mathbf{0}$ and $\boldsymbol{E}_{\mathcal{G},a}^3 = \mathbf{0}$. Also (16f) gives $\boldsymbol{P}_\mathcal{E}^2 = \mathbf{0}$ since the line switch status makes $\mathcal{V}_a$ isolated. Then, it follows from (16b) that $\sum_{i \in \mathcal{V}_a} P_i^{pre} = \mathbf{1}_a^T \boldsymbol{E}_{\mathcal{G},a} \boldsymbol{P}_\mathcal{E} = \mathbf{1}_a^T \boldsymbol{E}_{\mathcal{G},a}^1 \boldsymbol{P}_\mathcal{E}^1 + \mathbf{1}_a^T \boldsymbol{E}_{\mathcal{G},a}^2 \boldsymbol{P}_\mathcal{E}^2 + \mathbf{1}_a^T \boldsymbol{E}_{\mathcal{G},a}^3 \boldsymbol{P}_\mathcal{E}^3 = 0$, which violates the precondition $\sum_{i \in \mathcal{V}_a} P_i^{pre} \neq 0$. Therefore, these two types of configurations are excluded by constraints (16b), (16f), (16k) and (16l) and the sufficiency holds. ■

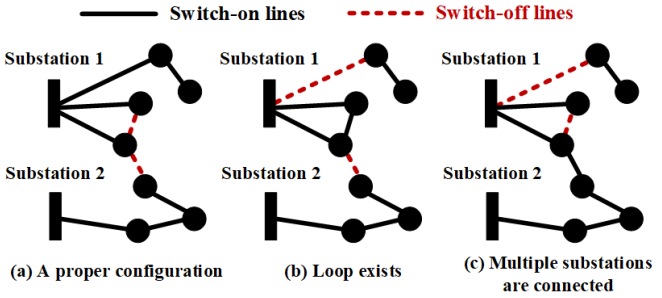

Figure 2. Three types of configurations satisfying (16k) and (16l).

The precondition $\sum_{i \in \mathcal{V}_a} P_i^{pre} \neq 0$ in Theorem 1 usually holds true since the active power loads and active power outputs of DGs in a subregion of the distribution system are not perfectly balanced. A possible exception is that all the buses in a subregion have zero power injections. In this case, we can add very small fictitious loads to those buses for the satisfaction of the precondition, which imposes negligible impact on the actual power flow and voltage profile. The proposed radiality constraint can be regarded as an improved version of [19]. In [19], a fictitious flow network with the same topology as the distribution system is introduced, and the network radiality is indirectly imposed by balancing the sources and sinks in this flow network. By comparison, we describe the radiality condition in a similar and more direct

way by utilizing the existing power flows, which lowers problem dimension.

In general, the solution to (16) provides a good set point that balances economy and voltage regulation. We have less network loss and near-flat voltage profile if the DG outputs go as predicted. Otherwise, the voltage volatility constraints guarantee that voltage deviations are kept within an acceptable range even though the power injections are fluctuating. As a consequence, the cost of corrective voltage control, which is mainly by power electronic devices, can be significantly saved. This suggests that network reconfiguration has unique value in handling the voltage volatility problem. Also, we point out that the proposed formulation is substantially different from the robust optimization that prevents voltage violation given an uncertainty interval of power injections (e.g., see [20]). Robust optimization is oriented to the worst scenario in the uncertainty interval, which requires that the interval is not too wide to render an infeasible problem. In contrast, the mechanism behind (16) is to reduce the risk of voltage violation by "strengthening" the distribution network structure. It is scenario-independent and works properly regardless of the uncertainty information that may be hard to obtain in real situations.

The proposed formulation refers to the static reconfiguration with respect to a single system snapshot. Given a typical load and DG output scenario, it can be used to determine the network structure and CB compensation for a weekly or monthly time frame. Nevertheless, this formulation has high potential for future development. For instance, given daily load and DG curves, problem (16) can be extended to a dynamic reconfiguration that determines hourly schemes for network structure and CBs, possibly with additional coupling constraints for the concerned time slots. Also, it will add more practicality if problem (16) can be extended to unbalanced three-phase distribution systems. To this end, we may resort to a linear version of the three-phase power flow equations (e.g., see [21]) to generalize the definition of voltage volatility index. These directions will be considered in future work.

B. Solution method

Due to constraint (16n), problem (16) is a general mixed-integer nonlinear programming (MINLP), which is hard to solve. On the other hand, the optimization problem excluding (16n) is a mixed-integer quadratic programming (MIQP), where sophisticated solvers are available. This property facilitates the application of Benders decomposition approach to problem (16). Benders decomposition has been widely used to solve MINLPs in power systems such as transmission switching [22], network reconfiguration [20, 23] and unit commitment [24, 25]. Generally, it decomposes a complex original problem into a master problem and a few subproblems that are much easier to solve. After obtaining the optimal solution to the master problem, the subproblems check if the solution is feasible for the original problem. In case of constraint violations, the corresponding Benders cuts are added to the master problem, and the optimal solution to the master problem is updated. The iteration stops when all constraints are satisfied.

For problem (16), we set the master problem to consist of (16a)-(16m). As aforementioned, the master problem is an MIQP. Denote the optimal solution to the master problem as $(\boldsymbol{\alpha}^*, \boldsymbol{c}^*, \boldsymbol{V}_d^*, \boldsymbol{P}_{\mathcal{E}}^*, \boldsymbol{Q}_{\mathcal{E}}^*)$. The subproblem checks if the voltage volatility constraints (16n) are satisfied by the solution. If there exists a subset of buses $\mathcal{V}_d' \subseteq \mathcal{V}_d$ such that $\mathcal{I}_i(\boldsymbol{\alpha}^*) > \mathcal{I}_i^{\max}$, $\forall i \in \mathcal{V}_d'$, we find bus m with the most severe violation by

$$m = \arg\min_{i \in \mathcal{V}_d'} \ \mathcal{I}_i^{\max} - \mathcal{I}_i(\boldsymbol{\alpha}^*) \tag{17}$$

and the corresponding Benders cut is formulated by

$$\mathcal{I}_m(\boldsymbol{\alpha}^*) + (\frac{\Delta \mathcal{I}_m}{\Delta \boldsymbol{\alpha}})^T(\boldsymbol{\alpha} - \boldsymbol{\alpha}^*) \le \mathcal{I}_m^{\max} \tag{18}$$

where $\frac{\Delta \mathcal{I}_m}{\Delta \boldsymbol{\alpha}} = [\frac{\Delta \mathcal{I}_m}{\Delta \alpha_{ij}}] \in \mathbb{R}^l$, $\forall (i,j) \in \mathcal{E}$. By using (15), the sensitivity $\frac{\Delta \mathcal{I}_m}{\Delta \alpha_{ij}}$ can be calculated by (assume $\Delta \alpha_{ij} = 1$)

$$\begin{aligned}
\frac{\Delta \mathcal{I}_m}{\Delta \alpha_{ij}} &= \boldsymbol{e}_m^T \frac{[\boldsymbol{R}(\boldsymbol{\alpha}^*)^{-1} + \Delta\alpha_{ij} r_{ij}^{-1} \boldsymbol{E}_{ij} \boldsymbol{E}_{ij}^T]^{-1}}{\Delta \alpha_{ij}} \boldsymbol{e}_{dg} \\
&\quad + \boldsymbol{e}_m^T \frac{[\boldsymbol{X}(\boldsymbol{\alpha}^*)^{-1} + \Delta\alpha_{ij} x_{ij}^{-1} \boldsymbol{E}_{ij} \boldsymbol{E}_{ij}^T]^{-1}}{\Delta \alpha_{ij}} \boldsymbol{e}_{dg} \\
&\quad - \boldsymbol{e}_m^T \frac{\boldsymbol{R}(\boldsymbol{\alpha}^*) + \boldsymbol{X}(\boldsymbol{\alpha}^*)}{\Delta \alpha_{ij}} \boldsymbol{e}_{dg} \\
&= -\frac{r_{ij}^{-1} \boldsymbol{e}_m^T \boldsymbol{R}(\boldsymbol{\alpha}^*) \boldsymbol{E}_{ij} \boldsymbol{E}_{ij}^T \boldsymbol{R}(\boldsymbol{\alpha}^*) \boldsymbol{e}_{dg}}{1 + r_{ij}^{-1} \boldsymbol{E}_{ij}^T \boldsymbol{R}(\boldsymbol{\alpha}^*) \boldsymbol{E}_{ij}} \\
&\quad - \frac{x_{ij}^{-1} \boldsymbol{e}_m^T \boldsymbol{X}(\boldsymbol{\alpha}^*) \boldsymbol{E}_{ij} \boldsymbol{E}_{ij}^T \boldsymbol{X}(\boldsymbol{\alpha}^*) \boldsymbol{e}_{dg}}{1 + x_{ij}^{-1} \boldsymbol{E}_{ij}^T \boldsymbol{X}(\boldsymbol{\alpha}^*) \boldsymbol{E}_{ij}}
\end{aligned} \tag{19}$$

where $\boldsymbol{E}_{ij} \in \mathbb{R}^d$ is a column of $\boldsymbol{E}_{\mathcal{G},d} \in \mathbb{R}^{d \times l}$ that is with respect to line (i,j). The Sherman-Morrison formula is employed in the derivation of (19) and we refer to [26] for the details. Then, the master problem is solved iteratively with Benders cut (18) being included as an additional constraint, which is still an MIQP. The inclusion of (18) helps to modify the current configuration $\boldsymbol{\alpha}^*$ in such a way that the voltage volatility constraint of bus m will be satisfied.

We summarize the solution procedure as follows. The corresponding flow chart is shown in Fig. 3.

Step 1: Solve the master problem consisting of (16a)-(16m) and obtain the initial solution.

Step 2: Check if the voltage volatility constraints (16n) are all satisfied at the current solution. If so, stop the algorithm, the current solution is the optimal solution to problem (16). Otherwise, go to Step 3.

Step 3: Find the bus with the most severe violation on voltage volatility constraint by (17), generate the corresponding Benders cut (18) and add it to the master problem.

Step 4: Solve the current master problem, update the current solution, and go back to Step 2.

Given a distribution system with s substations, d non-substation buses (with d_{cb} buses installing CBs) and l total lines (with l_{sw} lines being switchable), each MIQP master problem to be solved during the iteration has $d+2l$ continuous decision variables, $d_{cb} + l_{sw}$ integer decision variables and $3d + 4l + s + d_{cb} + l_{sw} + n_{cut} + 1$ constraints, where n_{cut} is a small number representing the number of added Benders cuts. Although the problem dimension grows linearly with system

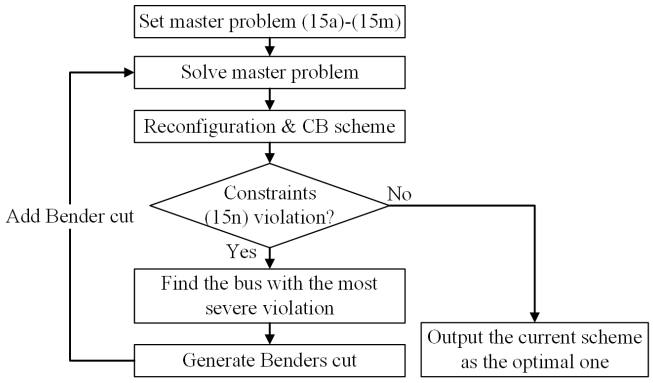

Figure 3. Flow chart of the solution method.

size, the NP-complete nature of mixed-integer programming [27] inevitably makes it computationally intractable when applied to large systems. It should be noted that the low scalability is an inherent feature of reconfiguration problems. We observe that the solution process for large systems (e.g., with more than 100 integer variables) could be highly time-consuming even without considering voltage volatility constraints. This case ends up with a sub-optimal solution as the optimality gap does not converge zero when the maximum computation time (e.g., 1800 seconds per master problem) is reached. The details are not shown here as they are similar to the common failing reported in the literature [2, 3].

Nevertheless, the proposed algorithm is shown to be adequate for medium-size systems. It will be seen in the case study that the algorithm efficiently solves problem (16) for the IEEE 69-bus system, and the obtained reconfiguration scheme performs well in reducing voltage volatility and network loss as expected. Therefore, the proposed formulation, which exploits the capability of network reconfiguration in addressing the voltage volatility issue, has unique merits despite its inherent complexity. On the other hand, to facilitate the application to systems with a large number of switches or dynamic reconfiguration with coupled switch actions during a long time span, future works should consider enhancing the solution method by combining the strength of other kinds of optimization methods such as heuristic and evolutionary computation.

V. Case Study

A. Test system & solution process

Take the IEEE 69-bus system shown in Fig. 4 to test the proposed method, where the line parameters are the same as those in [28] and the loads are 1.5 times of those in [28] to create a heavy load scenario. The impedances of the five lines that are initially switched off are all set to be $1.0 + \mathrm{j}1.0$ p.u.. Twelve renewable DGs and five CBs are added to those regions with heavy loads. Assume each DG operates at the unity power factor, which is a common scenario for renewable resources considered in the literature [29, 30]. The predicted DG outputs are given in Table I. Each CB consists of five units with the unit size being 0.2 MVar. Note that the total active power load is 5.703 MW, so the system has a high level of renewable penetration around 72%.

The parameter settings for solving problem (16) are listed as follows. All lines are switchable so that they can participate in the reconfiguration (i.e., $\mathcal{E}_{sw} = \mathcal{E}$), which is a common assumption [2]. A tighter voltage bound $V_i^{\min} = 0.97$, $V_i^{\max} = 1.03$ is adopted for those end-point buses 26, 27, 64, 65 for a better control effect, and a normal bound $V_i^{\min} = 0.95$, $V_i^{\max} = 1.05$ for the remaining non-substation buses. The substation bus keeps constant voltage $V_i = 1.0$. In addition, we set $\mathcal{I}_i^{\max} = 30$ for each non-substation bus that aims to reduce by half of the volatility as in the original network configuration.

The optimization computation is carried out on a computer with Intel Core i5-4570 CPU 3.20GHz, RAM 8.00 GB and 64-bit operating system. CPLEX is taken as the solver for each MIQP master problem during the Benders decomposition-based iteration. The proposed reconfiguration scheme is obtained after seven iterations. It takes around 15 seconds to solve each master problem, and the total computation time is 125.2 seconds. The solution process is fast considering that each master problem during the iteration consists of 214 continuous decision variables, 78 integer decision variables and 576-582 constraints (depending on number of iteration).

In summary we obtain the following three network configurations from the solution process:

- The *original network* configuration shown in Fig. 4;
- The *traditional reconfiguration scheme* that only aims to reduce network loss, which is the initial solution during the iteration;
- The *proposed reconfiguration scheme*, which is obtained by solving problem (16).

The details of the three schemes are listed in Table II, and the corresponding voltage volatility profiles are depicted in Fig. 5. We observe that $\mathcal{I}_i \leq 30$ is satisfied by each bus under the proposed reconfiguration scheme, which shows the effectiveness of voltage volatility constraints in problem (16). A detailed analysis will be given in the next subsection.

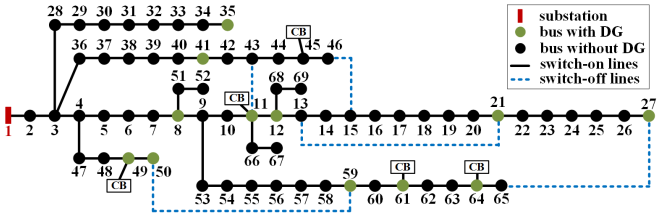

Figure 4. Diagram of the IEEE 69-bus system.

Table I
Predicted DG outputs (MW)

Bus	P_G	Bus	P_G	Bus	P_G	Bus	P_G
8	0.18	21	0.18	41	0.18	59	0.18
11	0.36	27	0.18	49	0.36	61	1.08
12	0.36	35	0.18	50	0.36	64	0.54

Table II
DETAILS OF THE THREE NETWORK CONFIGURATIONS

	Original network	Traditional reconfig.	Proposed reconfig.
Network loss	0.318 MW	0.0195 MW	0.0196 MW
CB at bus 11	0	0.60 MVar	0.80 MVar
CB at bus 45	0	0.20 MVar	0.20 MVar
CB at bus 49	0	1.00 MVar	1.00 MVar
CB at bus 61	0	1.00 MVar	1.00 MVar
CB at bus 64	0	0.60 MVar	0.60 MVar
Switch-off lines	(11,43), (13,21) (15,46), (50,59) (27,65)	(9,10),(13,14) (19,20),(58,59) (11,43)	(14,15),(18,19) (26,27),(58,59) (11,43)

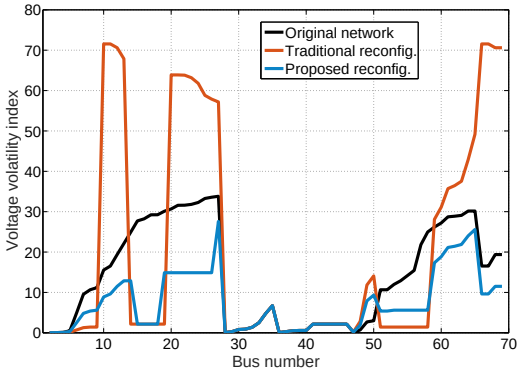

Figure 5. Voltage volatility under the three network configurations.

B. Performance of proposed reconfiguration scheme

We show the merits of the proposed reconfiguration scheme by comparing it with the original network and traditional reconfiguration scheme from the following aspects.

1) Network loss. The power flow profiles under the three schemes are depicted in Fig. 6, Fig. 7 and Fig. 8, respectively. We observe that quite a few lines have heavy power flows in the original network (see the lateral branch from bus 53 to bus 65 in Fig. 6), which is not economic. This is mainly caused by the original network not closely matching the load allocation. Buses 53-60 have light loads, but buses 61-65 have heavy loads that cannot be fully fed by the nearby DGs. So a large amount of power has to flow from the substation to buses 61-65, which causes large network loss (see Table II). In the traditional reconfiguration scheme and proposed reconfiguration scheme, this problem is solved by switching off line (58, 59) and switching on line (50, 59). By doing so, the power flow from bus 53 to bus 58 are much decreased since the heavy loads at buses 61-65 are fed by other paths with more nearby DGs, which leads to considerable loss reduction. In addition, the traditional scheme has smaller network loss than the proposed scheme as it does not consider voltage volatility constraints; nevertheless, the difference is not significant.

2) Voltage volatility. As shown in Fig. 5, the traditional reconfiguration, which aims at network loss reduction only, renders a dangerous voltage volatility level that is much higher than the original network. Note that lines (50, 59) and (27, 65) are switched on, and lines (58, 59) and (9,10) are switched off in the traditional reconfiguration scheme (see Fig. 7). As mentioned before, this operation improves the power flow distribution. Meanwhile, it also creates a long lateral branch from bus 47 to bus 10 that contains nine DGs, which leads to high voltage volatility of buses 10-13, 20-27, 65-70. By comparison, the proposed reconfiguration scheme prevents such a long lateral branch by disconnecting line (26,27) and reconnecting line (9, 10), which significantly reduces the voltage volatility level. In addition, this change on line switch status has almost no impact on power flow profile as Fig. 7 and Fig. 8 show that only the line flow from bus 59 to bus 61 is slightly increased. So the proposed reconfiguration scheme achieves both high economy and low voltage volatility.

3) Relationship between network loss and voltage volatility. We summarize the feature of the three schemes in Table III, which leads to some interesting observations that necessitate the proposed reconfiguration scheme:

(a) There is no clear monotonic relationship between network loss and voltage volatility.
(b) Voltage volatility level could be surprisingly high for a reconfiguration scheme only focusing on minimizing network loss.
(c) Voltage volatility level could be significantly reduced by a small percentage of extra network loss, if network reconfiguration is properly implemented by, e.g., the proposed formulation.

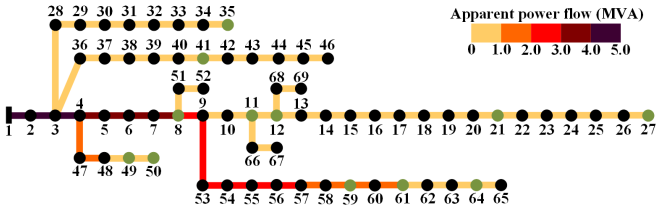

Figure 6. Power flow profile of the original network.

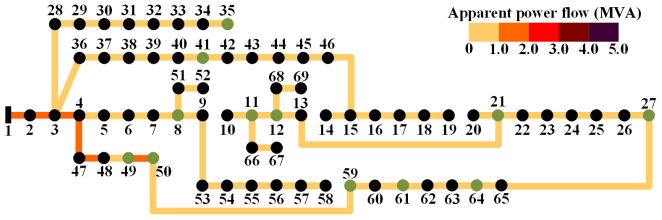

Figure 7. Power flow profile of the traditional reconfiguration scheme.

Table III
FEATURE SUMMARY OF THE THREE NETWORK CONFIGURATIONS

	Original network	Traditional reconfig.	Proposed reconfig.
Network loss	high	low	low (slightly greater than traditional one)
Voltage volatility	medium	high	low

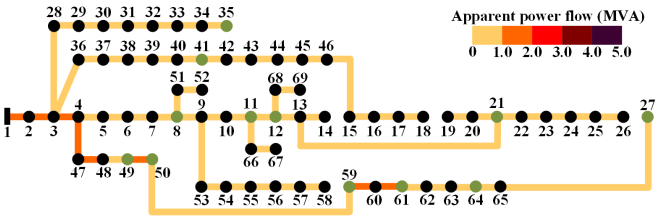

Figure 8. Power flow profile of the proposed reconfiguration scheme.

The merits of the proposed reconfiguration scheme can be further shown by the following experiments. For each DG, we simulate its output fluctuation by multiplying a factor η_i to the predicted value, where η_i independently follows the normal distribution with the mean being one and standard deviation being 25%. Then, we randomly choose 5000 DG output scenarios, and obtain the corresponding exact voltage profiles under the three schemes by solving the nonlinear power flow equations. The results are depicted in Fig. 9, Fig. 10 and Fig. 11, respectively.

Although the original network configuration has a rather low voltage volatility level (see Fig. 5), Fig. 9 shows that voltage violations occur in most of the scenarios as this configuration leads to an unsatisfactory low voltage profile at base case (see the black dash curve). The traditional reconfiguration scheme gets a good base voltage profile that is nearly flat. However, as shown in Fig. 10, voltage violations are still likely to occur, and the buses with frequent violations well correspond to those with high voltage volatility level. By comparison, Fig. 11 clearly shows the effect of voltage volatility constraints in the proposed reconfiguration scheme. The voltage deviations are restricted to a much narrower range so that no voltage violations are observed. In addition, Fig. 12 depicts the empirical probability density functions of the voltages of bus 26 and bus 66 from the 5000 samplings. The two selected buses are among those with high voltage volatility in the traditional reconfiguration scheme. Fig. 12 details the effect of the proposed reconfiguration scheme in mitigating the voltage volatility of certain buses. The shapes of these probability density functions further confirm the volatility evaluation by the proposed index shown in Fig. 5.

Moreover, we select one of the 5000 DG output scenarios shown in Table IV, which causes severe voltage violations under the traditional reconfiguration scheme. To eliminate voltage violations in this case, we have to resort to corrective control by power electronic controllers. The minimum additional reactive power support from power electronic controllers can be estimated by the following problem

$$\begin{aligned} \min_{\Delta \boldsymbol{Q}_d} \ & \sum\nolimits_{i\in\mathcal{V}_d} |\Delta Q_i| \\ s.t. \ & \boldsymbol{V}_d = \boldsymbol{R}\boldsymbol{P}_d + \boldsymbol{X}(\boldsymbol{Q}_d + \Delta\boldsymbol{Q}_d) + \boldsymbol{V}_d^0 \\ & \boldsymbol{V}_d^{\min} \le \boldsymbol{V}_d \le \boldsymbol{V}_d^{\max} \end{aligned} \tag{20}$$

where $\Delta\boldsymbol{Q}_d = [\Delta Q_i] \in \mathbb{R}^d$, $\forall i \in \mathcal{V}_d$ denotes the vector of additional reactive power injections, $\boldsymbol{P}_d, \boldsymbol{Q}_d$ refer to power injections in the selected scenario, $\boldsymbol{R}, \boldsymbol{X}$ refer to the network topology under the traditional reconfiguration scheme. Note that problem (20) provides the most optimistic estimation as it assumes power electronic controller is available at every bus. We set $V_i^{\min} = 0.97$, $V_i^{\max} = 1.03$, $\forall i \in \mathcal{V}_d$ in (20) that aims to achieve a similar voltage profile to the one under the proposed reconfiguration scheme with the same DG outputs. It turns out that we need at least 0.46 MVar total amount of additional reactive power from power electronic controllers, which implies a considerable investment on power electronic devices. This again highlights the performance of the proposed reconfiguration scheme as all voltage profiles in Fig. 11 are satisfactory even without any additional control.

From the above discussion, we conclude that the proposed formulation exploits the power of network reconfiguration in reducing or even preventing the risk of voltage violations with the presence of volatile DGs. Also we can expect much higher hosting capacity of renewable energy and lower investment and control complexity of power-electronic voltage controllers under this new framework.

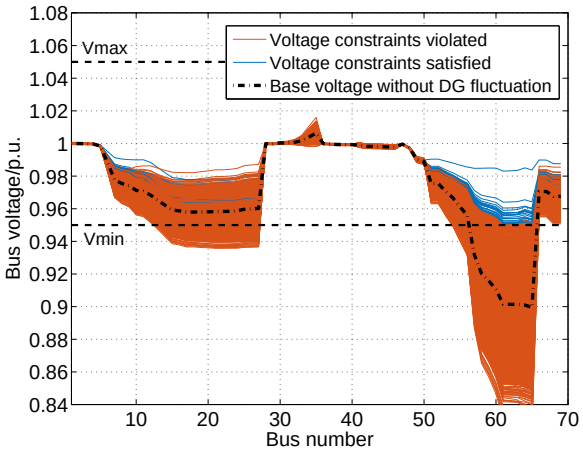

Figure 9. The original network: bus voltages under volatile DG outputs.

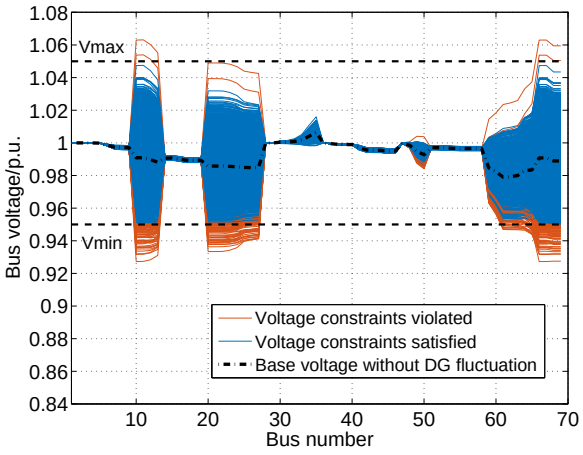

Figure 10. Traditional reconfiguration scheme: bus voltages under volatile DG outputs.

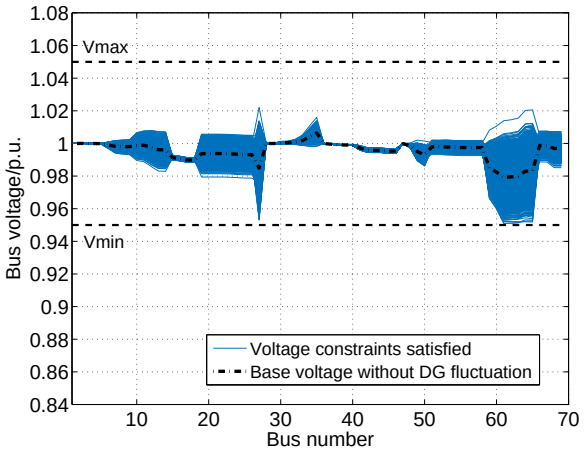

Figure 11. Proposed reconfiguration scheme: bus voltages under volatile DG outputs.

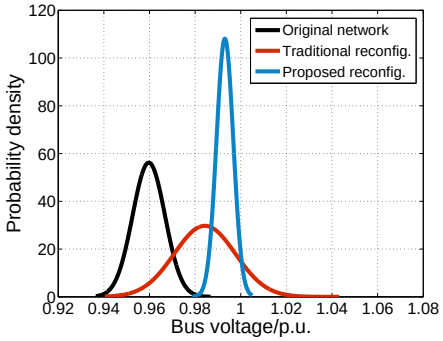

(a) Voltage of bus 26.

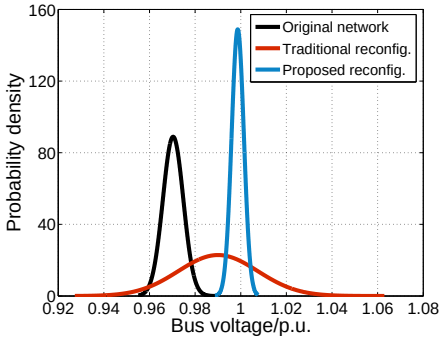

(b) Voltage of bus 66.

Figure 12. Probability density functions of bus voltages.

Table IV
DG OUTPUTS IN THE SELECTED SCENARIO (MW)

Bus	P_G	Bus	P_G	Bus	P_G	Bus	P_G
8	0.156	21	0.058	41	0.194	59	0.141
11	0.096	27	0.190	49	0.276	61	0.865
12	0.249	35	0.137	50	0.351	64	0.477

VI. CONCLUDING REMARKS AND FUTURE DIRECTIONS

We have developed a new network reconfiguration formulation that addresses the DG-induced voltage volatility in distribution systems. First, we have proposed a novel index to measure the voltage volatility of each bus based on the linear DistFlow equations. This voltage volatility index is a function of the distribution network structure that concisely describes the influence of DG output fluctuations on bus voltages. Then, we have established a new optimization model which coordinates the network reconfiguration and switched CBs to minimize network loss under a bounded voltage volatility level. This model is solved by the Benders decomposition-based algorithm. Numerical tests on the IEEE 69-bus system show that network reconfiguration may cause a highly volatile voltage profile if it only focuses on network loss reduction. On the other hand, the reconfiguration scheme obtained by the proposed model performs well in reducing both network loss and risk of voltage violations. The proposed method provides a fresh perspective that network reconfiguration can make an important contribution to the voltage regulation problem under volatile distributed generation.

It should be noted that the main objective of this paper is to confirm the feasibility and large potential of network reconfiguration in mitigating DG-induced voltage volatility. The proposed method is still preliminary in terms of modeling and solution methodology. Many future directions can be considered to make it more complete and practical. For instance, it needs to be extended to unbalanced three-phase networks, which is a more general operating scenario for distribution systems. The dynamic coordination between reconfiguration and existing power electronic controllers in the system also has potential benefits. Moreover, the solution method needs to be further developed to promote large system application.

REFERENCES

[1] M. E. Baran and F. F. Wu, "Network reconfiguration in distribution systems for loss reduction and load balancing," *IEEE Trans. Power Del.*, vol. 4, no. 2, pp. 1401–1407, April 1989.

[2] R. A. Jabr, R. Singh, and B. C. Pal, "Minimum loss network reconfiguration using mixed-integer convex programming," *IEEE Trans. Power Syst.*, vol. 27, no. 2, pp. 1106–1115, May 2012.

[3] J. A. Taylor and F. S. Hover, "Convex models of distribution system reconfiguration," *IEEE Trans. Power Syst.*, vol. 27, no. 3, pp. 1407–1413, August 2012.

[4] A. Ahuja, S. Das, and A. Pahwa, "An AIS-ACO hybrid approach for multi-objective distribution system reconfiguration," *IEEE Trans. Power Syst.*, vol. 22, no. 3, pp. 1101–1111, August 2007.

[5] A. Asrari, S. Lotfifard, and M. Ansari, "Reconfiguration of smart distribution systems with time varying loads using parallel computing," *IEEE Trans. Smart Grid*, vol. 7, no. 6, pp. 2713–2723, November 2016.

[6] A. Kavousi-Fard and T. Niknam, "Optimal distribution feeder reconfiguration for reliability improvement considering uncertainty," *IEEE Trans. Power Del.*, vol. 29, no. 3, pp. 1344–1353, June 2014.

[7] V. Madani, R. Das, F. Aminifar, J. McDonald, S. Venkata, D. Novosel, A. Bose, and M. Shahidehpour, "Distribution automation strategies challenges and opportunities in a changing landscape," *IEEE Trans. Smart Grid*, vol. 6, no. 4, pp. 2157–2165, July 2015.

[8] M. Cramer, C. Matrose, M. Cremer, A. Schnettler, P. Hahulla, and T. Smolka, "Voltage and power characteristics in German low voltage grids: Field experience in presence of high photovoltaic installations and voltage-regulated distribution transformers (VRDT)," in *Proc. IET Intl. Conf. Renewable Power Gener.*, September 2016, pp. 1–6.

[9] F. Capitanescu, L. F. Ochoa, H. Margossian, and N. D. Hatziargyriou, "Assessing the potential of network reconfiguration to improve distributed generation hosting capacity in active distribution systems," *IEEE Trans. Power Syst.*, vol. 30, no. 1, pp. 346–356, January 2015.

[10] N. C. Koutsoukis, D. O. Siagkas, P. S. Georgilakis, and N. D. Hatziargyriou, "Online reconfiguration of active distribution networks for maximum integration of distributed generation," *IEEE Trans. Autom. Sci. Eng.*, vol. 14, no. 2, pp. 437–448, April 2017.

[11] J. M. Bloemink and T. C. Green, "Benefits of distribution-level power electronics for supporting distributed generation growth," *IEEE Trans. Power Del.*, vol. 28, no. 2, pp. 911–919, April 2013.
[12] M. Farivar, L. Chen, and S. H. Low, "Equilibrium and dynamics of local voltage control in distribution systems," in *Proc. IEEE Conf. Dec. Control*, 2013, pp. 4329–4334.
[13] Y. Zheng, D. J. Hill, K. Meng, and S. Y. Hui, "Critical bus voltage support in distribution systems with electric springs and responsibility sharing," *IEEE Trans. Power Syst.*, vol. 32, no. 5, pp. 3584–3593, September 2017.
[14] A. Parchure, S. J. Tyler, M. A. Peskin, K. Rahimi, R. P. Broadwater, and M. Dilek, "Investigating PV generation induced voltage volatility for customers sharing a distribution service transformer," *IEEE Trans. Ind. Appl.*, vol. 53, no. 1, pp. 71–79, Jan.-Feb 2017.
[15] K. Jhala, B. Natarajan, and A. Pahwa, "Probabilistic voltage sensitivity analysis (PVSA)—a novel approach to quantify impact of active consumers," *IEEE Trans. Power Syst.*, vol. 33, no. 3, pp. 2518–2527, May 2018.
[16] K. Jhala, B. Natarajan, and A. Pahwa, "Probabilistic voltage sensitivity analysis (PVSA) for random spatial distribution of active consumers," in *Proc. IEEE Innov. Smart Grid Tech. Conf.*, 2018, pp. 1–5.
[17] R. B. Bapat, *Graphs and Matrices*. Springer, 2010.
[18] C. Guan, P. B. Luh, L. D. Michel, Y. Wang, and P. B. Friedland, "Very short-term load forecasting: wavelet neural networks with data prefiltering," *IEEE Trans. Power Syst.*, vol. 28, no. 1, pp. 30–41, February 2013.
[19] M. Lavorato, J. F. Franco, M. J. Rider, and R. Romero, "Imposing radiality constraints in distribution system optimization problems," *IEEE Trans. Power Syst.*, vol. 27, no. 1, pp. 172–180, February 2012.
[20] C. Lee, C. Liu, S. Mehrotra, and Z. Bie, "Robust distribution network reconfiguration," *IEEE Trans. Smart Grid*, vol. 6, no. 2, pp. 836–842, March 2015.
[21] L. Gan and S. H. Low, "Convex relaxations and linear approximation for optimal power flow in multiphase radial networks," in *Proc. Power Syst. Comput. Conf.*, 2014, pp. 1–9.
[22] M. Khanabadi, H. Ghasemi, and M. Doostizadeh, "Optimal transmission switching considering voltage security and N-1 contingency analysis," *IEEE Trans. Power Syst.*, vol. 28, no. 1, pp. 542–550, February 2013.
[23] H. Khodr, J. Martinez-Crespo, M. Matos, and J. Pereira, "Distribution systems reconfiguration based on OPF using Benders decomposition," *IEEE Trans. Power Del.*, vol. 24, no. 4, pp. 2166–2176, October 2009.
[24] J. Wang, M. Shahidehpour, and Z. Li, "Security-constrained unit commitment with volatile wind power generation," *IEEE Trans. Power Syst.*, vol. 23, no. 3, pp. 1319–1327, August 2008.
[25] Y. Xu, Z. Y. Dong, R. Zhang, Y. Xue, and D. J. Hill, "A decomposition-based practical approach to transient stability-constrained unit commitment," *IEEE Trans. Power Syst.*, vol. 30, no. 3, pp. 1455–1464, May 2015.
[26] W. W. Hager, "Updating the inverse of a matrix," *SIAM Review*, vol. 31, no. 2, pp. 221–239, 1989.
[27] M. R. Garey and D. S. Johnson, *Computers and Intractability: A Guide to the Theory of NP-Completeness*. W.H. Freeman and Company, New York, 1979.
[28] M. E. Baran and F. F. Wu, "Optimal capacitor placement on radial distribution systems," *IEEE Trans. Power Del.*, vol. 4, no. 1, pp. 725–734, February 1989.
[29] D. Q. Hung, N. Mithulananthan, and R. C. Bansal, "Analytical expressions for DG allocation in primary distribution networks," *IEEE Trans. Energy Convers.*, vol. 25, no. 3, pp. 814–820, Sep. 2010.
[30] A. Navarro-Espinosa and L. F. Ochoa, "Probabilistic impact assessment of low carbon technologies in LV distribution systems," *IEEE Trans. Power Syst.*, vol. 31, no. 3, pp. 2192–2203, May 2016.

Yue Song (M'14) received B.S. and M.S. degrees from Shanghai Jiao Tong University, China, in 2011 and 2014, respectively, and the Ph.D. degree from the University of Hong Kong, Hong Kong, China, in 2017, all in electrical engineering. He is currently a Postdoctoral Fellow at the Department of Electrical and Electronic Engineering, the University of Hong Kong. He received the Hong Kong Ph.D. Fellowship from the Research Grants Council of Hong Kong, and CLP Fellowship in Electrical Engineering from the University of Hong Kong during his Ph.D. studies. His research interests include stability analysis, optimization and control of energy network systems.

Yu Zheng (M'15) received the B.E. degree from Shanghai Jiao Tong University, China, in 2009, and the Ph.D. degree from the University of Newcastle, Australia, in 2015. He is currently a Senior Research Assistant with the University of Hong Kong, Hong Kong. He is also a Visiting Professor at the Changsha University of Science and Technology, Changsha, China. His research interests include power electronic applied in power systems, power system planning, and smart grid.

Tao Liu (M'13) received the B.E. degree from Northeastern University, China, in 2003 and the Ph.D. degree from the Australian National University, Australia, in 2011. He was a Research Fellow in the Research School of Engineering at the Australian National University from January 2012 to May 2012, during which he also held a visiting scholar position in the Centre for Future Energy Networks at the University of Sydney, Australia. From June 2012 to August 2013, he worked as a postdoctoral fellow at the University of Groningen, the Netherlands. He moved to the University of Hong Kong as a postdoctoral fellow in September 2013, and then became a Research Assistant Professor in June 2015. He is currently an Assistant Professor in the Department of Electrical and Electronic Engineering at the same University. His research interests include power systems, dynamical networks, distributed control, event-triggered control and switched systems.

Shunbo Lei (M'17) received the B.E. degree in electrical engineering from Huazhong University of Science and Technology, Wuhan, China, in 2013, and the Ph.D. degree in electrical and electronic engineering from the University of Hong Kong, Hong Kong, in 2017. He was a Visiting Scholar at Argonne National Laboratory, Argonne, IL, USA, from 2015 to 2016. He was a Postdoctoral Researcher with the University of Hong Kong, Hong Kong, from 2017 to 2019. He is currently a Research Fellow with the University of Michigan, Ann Arbor, MI, USA. His research interests include power system operation, resilience, demand response, convex optimization, and machine learning.

David J. Hill (M'76-SM'91-F'93-LF'14) received the B.E. (electrical engineering) and B.Sc. (mathematics) degrees from the University of Queensland, Australia, in 1972 and 1974, respectively. He received the Ph.D. degree in electrical engineering from the University of Newcastle, Australia, in 1976. He holds the Chair of Electrical Engineering with the Department of Electrical and Electronic Engineering, The University of Hong Kong, Hong Kong. He is also a part-time Professor and Director of the Centre for Future Energy Networks, The University of Sydney, Australia.

From 2005 to 2010, he was an Australian Research Council Federation Fellow with Australian National University. Since 1994, he has held various positions with the University of Sydney, Australia, including the Chair of Electrical Engineering until 2002 and from 2010 to 2013 along with an ARC Professorial Fellowship. He has also held academic and substantial visiting positions with the University of Melbourne, Australia, University of California, Berkeley, USA, University of Newcastle, Australia, Lund University, Sweden, University of Munich, Germany, City University of Hong Kong, Hong Kong, and Hong Kong Polytechnic University, Hong Kong. His general research interests are in control systems, complex networks, power systems and stability analysis. His work is now mainly on control and planning of future energy networks and basic stability and control questions for dynamic networks.

Prof. Hill is a Fellow of the Society for Industrial and Applied Mathematics, Philadelphia, PA, USA, the Australian Academy of Science, and the Australian Academy of Technological Sciences and Engineering. He is also a Foreign Member of the Royal Swedish Academy of Engineering Sciences.